ACTINOIDINS A AND A_2: STRUCTURE DETERMINATION USING 2D NMR METHODS

SARAH L. HEALD, LUCIANO MUELLER and PETER W. JEFFS

Smith Kline & French Laboratories,
709 Swedeland Road, Swedeland, PA 19479, U.S.A.

(Received for publication December 15, 1986)

The structural analysis of the intact glycopeptide antibiotics, actinoidins A (**1a**) and A_2 (**1b**), by two-dimensional ^1H NMR is described. The location of the single chlorine at the A3 position and the sites of attachment of the four carbohydrate substituents in actinoidin A are elucidated based on correlation spectroscopy (COSY), double quantum coherence experiments (DQCE), homonuclear Hartmann-Hahn experiments (HOHAHA) and nuclear Overhauser spectroscopy (NOESY). Similar 2D correlation and NOE NMR experiments are then performed on the novel analog, actinoidin A_2, to determine its structure. The structural difference between actinoidins A and A_2 is shown to reside in the presence of L-rhamnose in actinoidin A_2 in place of L-acosamine in actinoidin A. All questions concerning the stereochemistry of the chiral centers in both the heptapeptide core and the carbohydrate moieties in each of these antibiotics could be successfully addressed with the exception of GI′, the α-carbon on the *N*-terminal amino acid which is known to have the *R*-configuration from previous studies.

The actinoidins, first isolated from *Proactinomyces actinoides*, are members of the vancomycin-ristocetin class of glycopeptide antibiotics[1,2]. The aglycone (**1**) of actinoidin A (**1a**) has been shown to contain monodechlorovancomycinic acid ("A-B-C" residue)[3], actinoidinic acid ("D-E")[4,5], L-phenylalanine ("F") and D-4-hydroxyphenylglycine ("G")[6]. In addition, sugar analysis has identified the four carbohydrate components as D-glucose, D-mannose[7], 2,3,6-trideoxy-3-amino-L-*arabino*-pyranose (L-acosamine) and 2,3,6-trideoxy-3-amino-4-methoxy-L-*arabino*-pyranose (L-actinosamine)[8]. Two of the sugar units are attached to the aglycone as the disaccharide, 2-*O*-(L-acosaminyl)-D-glucopyranose[9]. Through sequential methylation and hydrolysis of the glycopeptide, D-mannose has been located on the actinoidinic acid fragment which restricts it to 3 possible sites of attachment (D3, D5 and E4), while the disaccharide has been placed at the 4-position in the vancomycinic acid residue on the B-ring phenol[10,11]. By default, this has left L-actinosamine at the benzylic hydroxyl group in either the "A" or "C" amino acid. As yet unresolved in the structure of actinoidin A are the location of the single chlorine substituent, the placement of the sugars and the determination of the configuration of each anomeric linkage.

Recently, an unidentified *Nocardia* sp. (SK&F AAJ-193) which produces actinoidin A as well as a novel analog, actinoidin A_2, was isolated at the SK&F Laboratories[12]. The presence of actinoidin A was confirmed by co-elution with authentic material on HPLC, isoelectric focusing and fast atom bombardment mass spectrometry. Preliminary analysis of actinoidin A_2 indicated that it contains the same peptide core as actinoidin A along with the four sugars; D-glucose, D-mannose, L-rhamnose and L-actinosamine. In previous work on the complete 3-dimensional structure determination of aridicin[13] and the conformational analysis of teicoplanin A_2[14~17], we described an integrated approach to the elucidation of primary and tertiary structure of intact glycopeptides using two-dimensional (2D) NMR in conjunction with computer-assisted molecular modeling.

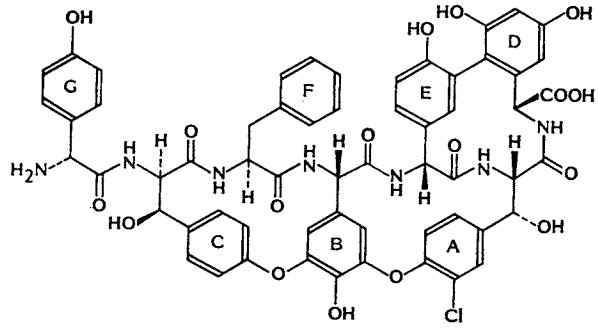

1

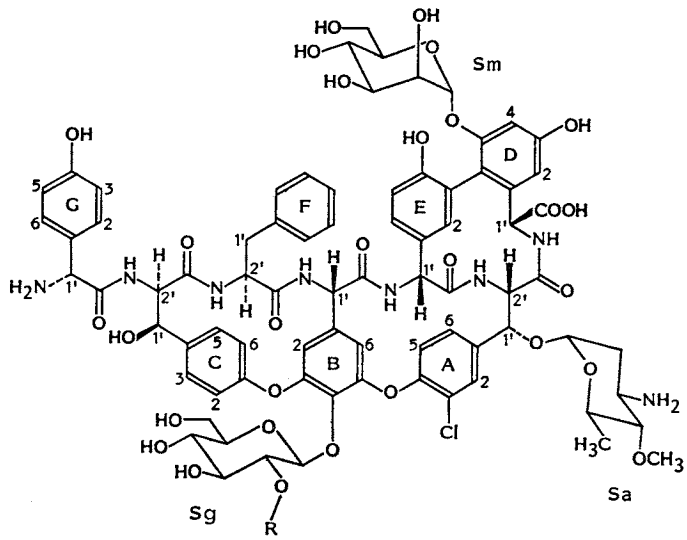

Actinoidin A (**1a**) R = 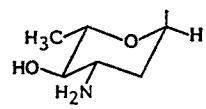 Sa'

Actinoidin A_2 (**1b**) R = 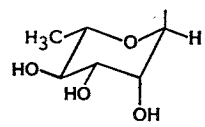 Sr

As a result of the experience gained with the NMR studies of aridicin and teicoplanin, we were in a position to undertake an investigation of the structures of actinoidins A and A_2 without the need to resort to methods involving chemical degradation. In the course of the 2D NMR analysis of actinoidin A_2 it became apparent that, while most of the structural issues concerning the aglycone could be solved by applying the NMR methods employed previously, the critical point in the interpretation of the data on the antibiotic required the unambiguous assignment of all the sugar frequencies. This situation was exacerbated in the actinoidins by the presence of overlapping signals from four similar sugar residues and the usual problems associated with poorly resolved spectra in the intact antibiotics of this class. This lead to the use of a new proton correlation sequence originally proposed

by BRAUNSCHWEILER and ERNST[18], and recently refined by DAVIS and BAX[19,20], the homonuclear Hartmann-Hahn (HOHAHA) experiment. In the 2D form of this experiment, cross-peaks may be observed between all coupled protons in a carbon chain. This technique proved extremely successful in the analysis of the sugar residues.

Location of the Chlorine Substituent

Both actinoidins A and A_2 give adequately-resolved proton spectra at 500 MHz in DMSO-d_6. A complete list of the observed chemical shifts and coupling constants for **1a** and **1b** are given in Table 1. The assignments of the proton frequencies are made based on the results from correlation spectroscopy (COSY)[21,22], double quantum coherence[23,24], homonuclear Hartmann-Hahn[19,20] and 2D nuclear Overhauser effect (NOE) experiments[25]. The coupling constants are calculated from resolution-enhanced spectra.

Fig. 1 illustrates the downfield region of the COSY spectrum obtained from actinoidin A. All seven aromatic spin systems can be identified and are categorized as follows; two AB, two ABX, two AA'BB' and one AA'BB'C. Assignment of the B, D and E ring spin patterns are made from comparisons with the spectra of aridicin A and teicoplanin A_2. The phenyl group (AA'BB'C) in the phenylalanine residue is identified as the complex multiplet at ~6.9 ppm, while the *p*-hydroxylphenyl ring in the G residue gives rise to a pair of doublets at 6.71 and 7.26 ppm. This leaves only the A

Table 1. Chemical shifts and coupling constants for actinoidins A and A_2, and proton T_1-recovery times for actinoidin A.

Assignment	Actinoidin A			Actinoidin A_2	
	Chemical shift (ppm)	Coupling constant (Hz)	T_1-value (seconds)	Chemical shift (ppm)	Coupling constant (Hz)
A residue					
ANH	6.89	unres.	unres.	7.13	8.2
A2'	4.25	unres.	2.17	4.26	8.2
A1'	5.10	s	2.46	5.10	s
A2	7.86	1.4	3.12	7.86	2.1
A5	7.30	8.5	3.10	7.31	8.2
A6	7.36	1.8, 8.4	2.80	7.34	2.3, 8.6
B residue					
BNH	7.98	8.6	1.75	7.99	8.8
B1'	5.60	8.5	3.69	5.60	8.5
B2	5.65	unres.	4.11 (Sg1)	5.66	3.0
B6	5.16	1.4	4.03	5.15	2.1
C residue					
CNH	—	—	—	—	—
C2'	4.52	4.4	2.81	4.51	unres.
C1'	5.21	4.8	2.90	5.20	4.2
C2	7.06	1.8, 8.5	3.35	7.06	2.4, 8.4
C3	7.11	2.3, 8.4	3.84	7.12	2.3, 8.5
C5	7.22	2.0	2.59 (E2)	7.21	3.0, 8.3
C6	7.77	1.7, 8.2	2.53	7.77	2.1, 8.9
D residue					
DNH	8.56	5.4	2.49	8.64	6.2
D1'	4.45	6.6	3.70 (F2')	4.47	6.2
D2	6.51	1.8	4.38	6.47	2.4
D4	6.72	2.4	2.84 (G3/G5)	6.73	2.4

Table 1. (Continued)

Assignment	Actinoidin A			Actinoidin A_2	
	Chemical shift (ppm)	Coupling constant (Hz)	T_1-value (seconds)	Chemical shift (ppm)	Coupling constant (Hz)
E residue					
ENH	8.53	unres.	2.57	8.52	5.7
E1′	4.50	8.7	2.50	4.52	unres.
E2	7.19	2.4	2.54 (C5)	7.20	3.0
E5	6.80	8.3	3.68 (E6)	6.81	8.5
E6	6.84	1.8, 8.4	3.68 (E5)	6.83	2.0, 8.3
F residue					
FNH	7.26	unres.	unres.	7.26	9.1
F1′a	2.68	8.1, −13.7	1.14	2.68	8.3, −13.3
F1′b	2.56	8.9, −13.7	1.40 (Sa4)	2.56	8.3, −13.3
F2′	4.46	7.8, 8.5	3.70 (D1′)	4.45	8.3, 9.1
F2/3/5/6	6.88	7.5	2.46	6.88	8.0
F4	7.04	7.0	2.81	7.01	6.7
G residue					
GNH	—	—	—	—	—
G1′	4.37	s	1.96	4.37	s
G2/G6	7.26	8.5	2.40	7.26	9.1
G3/G5	6.71	8.9	2.96	6.71	9.1
Carbohydrates					
D-Mannose (Sm)					
Sm1	5.19	1.6	2.41	5.20	<1.4
Sm2	3.17	3.9	unres.	3.19	unres.
Sm3	3.20	3.4, 9.4	unres.	3.21	unres.
Sm4	3.39	9.2	unres.	3.40	9.3
Sm5/6a, 6b	3.47	unres.	unres.	3.47	unres.
D-Glucose (Sg)					
Sg1	5.64	8.3	2.28	5.66	7.1
Sg2	3.61	8.3	unres.	3.62	unres.
Sg3	3.47	8.5	unres.	3.42	unres.
Sg4	3.23	8.5	unres.	3.23	unres.
Sg5	3.29	9.1	unres.	3.29	unres.
Sg6a	3.71	10.7	unres.	3.72	unres.
Sg6b	3.47	unres.	unres.	3.47	unres.
L-Acosamine (Sa′) and L-rhamnose (Sr)					
Sa′1/Sr1	5.36	1.2, 2.3	1.50	5.17	<1.4
Sa′2a/Sr2	2.05	unres.	1.13	3.72	3.4
Sa′2b	1.55	unres.	0.95		
Sa′3/Sr3	3.05	unres.	unres.	3.49	9.6
Sa′4/Sr4	2.89	9.3	1.45	3.21	unres.
Sa′5/Sr5	4.18	4.8, 9.3	1.64	4.10	6.1, 9.2
Sa′6/Sr6	1.10	6.3	0.82	1.08	6.2
L-Actinosamine (Sa)					
Sa1	4.67	<1.4	2.00	4.73	2.4
Sa2a	2.08	unres.	1.13	2.15	2.7, 4.8
Sa2b	1.47	unres.	1.35	1.60	unres.
Sa3	3.25	unres.	unres.	3.38	10.2
Sa4	2.56	8.1	1.40 (F1′b)	2.75	9.7
Sa5	3.61	6.0, 9.2	unres.	3.65	6.2, 9.2
Sa6	1.16	5.9	0.97	1.19	6.2
$-OCH_3$	3.33	s	unres.	3.34	s

unres.: Unresolved signal.
s: Singlet.

Fig. 1. 2D Proton-proton correlation spectrum of the aromatic region of actinoidin A.

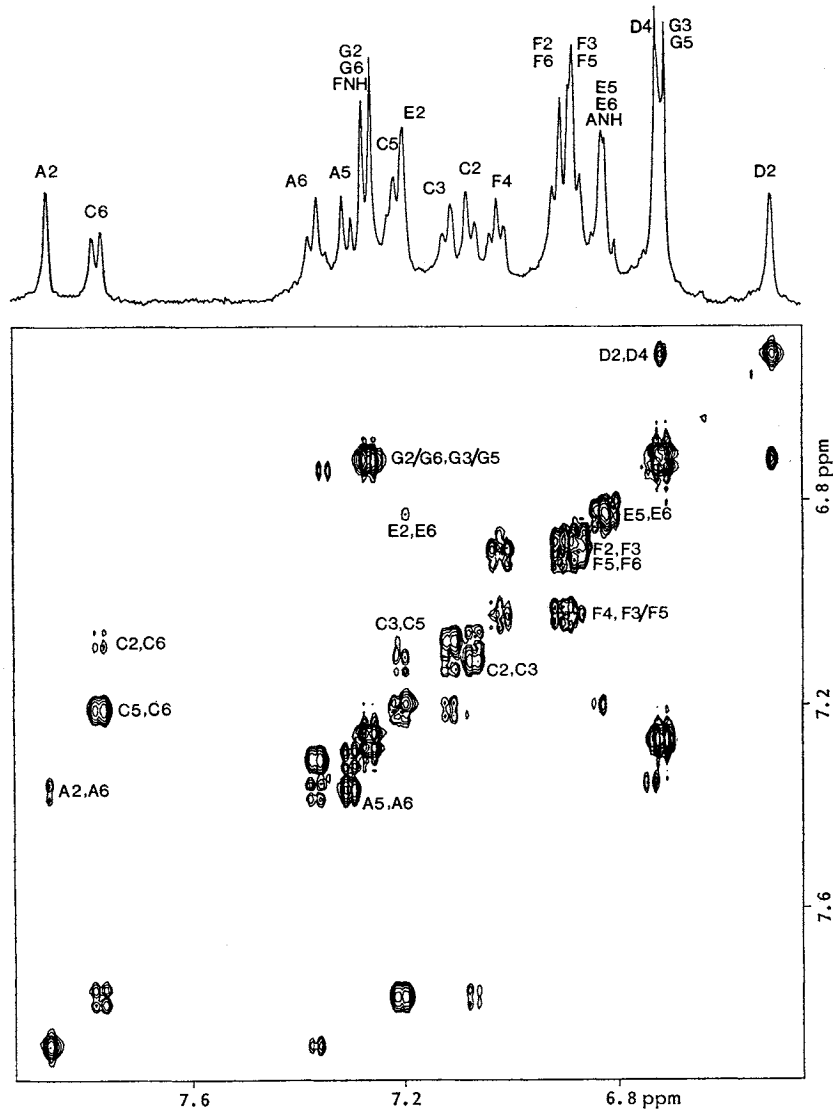

and C residues, which consequently are represented by ABX and AA′BB′ spin patterns. The specific assignments for the A and C residues can be made from consideration of the NOE interactions as explained in the following discussion.

A section of the 2D NOE spectrum which shows cross-peaks between the amide/aromatic frequencies and the α-peptide/anomeric sugar frequencies is presented in Fig. 2. The string of cross-peaks from the signal at δ 7.86, which is a member of the aromatic ABX pattern, confirms that this signal originates from A2 and establishes that the chlorine in actinoidin A is located at A3, as indicated in the partial structure **2**.

The assignment of aromatic protons belonging to the amino acid residues A, B, D and G was established by comparisons with spectra of the aglycones of aridicin and related members of the series[18~17]. In the case of the side-chain protons, a number of cross-peaks from long range couplings

Fig. 2. 2D Proton-proton nuclear Overhauser effect spectrum of actinoidin A showing cross-peaks between amide/aromatic hydrogens and the peptide α and anomeric sugar protons.

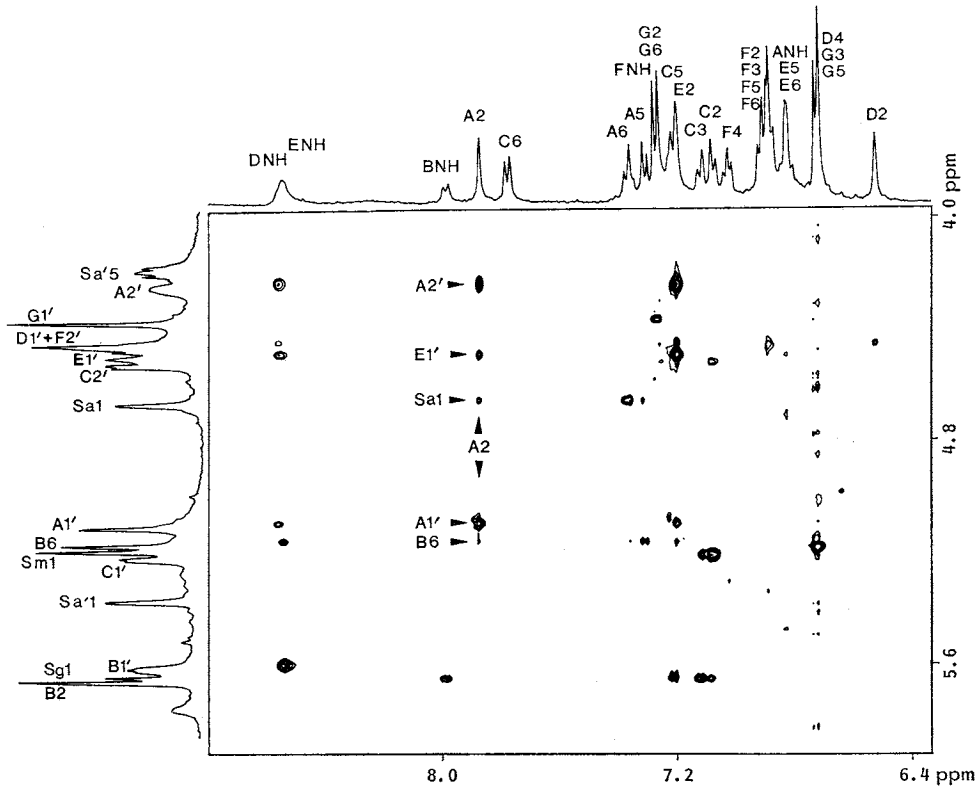

between benzylic and *ortho*-aromatic protons are observed in the delayed-COSY experiment and were utilized for making assignments. The remaining benzylic protons are assigned from the results obtained from a phase-sensitive 2D NOE experiment. The 2D NOE patterns are extensive enough so that each α-carbon proton can be positioned relative to neighboring amide and aromatic protons. The sequencing of the amino acid residues and linkages between aromatic rings are also confirmed by inspection of the 2D NOE patterns and comparison of these results to those previously observed for other members of this class of antibiotics. The chemical shifts and NOE patterns for the protons in the A, B, D and E residues are in excellent agreement with similar data obtained on teicoplanin A_2 in DMSO.

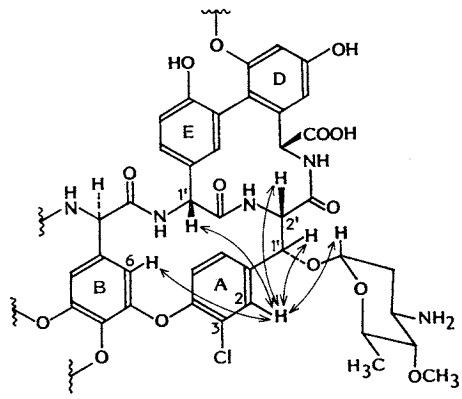

2

In common with the findings on other glycopeptide antibiotics of this series, the rigid nature of the macrocyclic peptide core prevents rings A and C from undergoing rotational flipping. Consequently, each of the four protons on ring C yields a distinct chemical shift and different NOE patterns which allows the orientation of the ring to be defined in relationship to the B ring and to the BNH/

FNH/CNH binding pocket. NOE cross-peaks involving C5 and C6 signals allow these protons to be aligned along the side of the binding pocket, while C3, C2, C1′ and C2′ are found on the outer face of the glycopeptide. Finally, C3 yields a stronger NOE to B2 than to C5 which indicates that C3 is closer to B2 than to C5. The overall NOE pattern is consistent with the relative configuration of the chiral centers in the B, C and F residues which has been previously established for other members of this class of antibiotics.

The increased mobility of the F and G residues as compared to these residues in aridicin and teicoplanin limits the conformational information which may be derived from the NOE experiments. The conformational mobility of the G ring and the absence of a terminal *N*-methyl group obviated the use of NMR for ascertaining the configuration of G1′. Fortunately the absolute stereochemistry at this site is known from chemical degradation experiments to have the *R*-configuration[6]. In addition, several lines of evidence indicate that the phenylalanine ring in the F residue has considerable mobility. A reflection of this situation is found in the similar values for the coupling constants between F1′a, F1′b and F2′ (see Table 1) indicate that the benzyl group is undergoing rapid rotation on the NMR line scale. Also, the NOE cross-peaks between F2′, F1′a, F1′b and the F ring yield distances which are all approximately equal indicating motional averaging. Moreover, these experimentally-derived distances derived from the intensities of the NOE's are longer than the theoretical distances for a rigid structure and are indicative of increased localized motion in this region of the molecule. This is also supported by the T_1-recovery times.

The T_1 values (see Table 1) for F1′a and F1′b protons are much shorter than those measured on the C5 and C6, the internal distance marker. Application of the PACHLER equations[26] to the coupling constants indicates that the phenylalanine side-chain rotamer populations are equally distributed between K=−60° and 180° positions.

Using the methods[14~17] described previously for teicoplanin A_2, interproton distances are calculated from quantitative NOE data in deriving a 3-dimensional structure. Table 2 is a partial list of these calculated distances which are considered to be approximate within the ranges indicated in the table.

The quality of the data for generating accurate coordinates from the NOE intensity measurements was not optimized. It was clear from the decrease in intensities in certain cross-peaks, including those resulting from A2/E1′ and A1′/Sa2a when the mixing time in the nuclear Overhauser spectroscopy (NOESY) experiment was reduced from 0.5 second to 0.3 second, that contributions to the intensities were occurring through spin diffusion. Provided this limitation is appreciated, the effects of spin diffusion assist in providing useful qualitative structural information. In view of these comments, it is felt that only the short distances (<3.0 Å) in Table 1 should be considered as reliable.

Location of the Sugar Substituents

In contrast to the heptapeptide core, elucidation of the structures of the carbohydrate components was more difficult. Not only are the carbohydrate proton resonances severely overlapped in DMSO solution, but the residual water in the sample occurs as a broad resonance peak superimposed on the sugar frequencies. Preliminary structural information was extracted from the COSY, double quantum, and NOESY experiments. For the two 6-deoxyamino sugars, L-acosamine and L-actinosamine, two separate sets of signals can be identified by initiating assignments from the sugar(S)6 methyl signals which appear at δ 1.16 and 1.10. In both cases strong coupling cross-peaks are observed in the COSY

Table 2. NOE distance calculations for peptide core of actinoidins A and A_2.

Cross-peak	Teicoplanin[a] (Å) mt[c] 500 PD[d] 4.0	Actinoidin A[b] (Å) mt 300 PD 15.0	Actinoidin A[b] (Å) mt 500 PD 2.5	Actinoidin A_2 (Å) mt 500 PD 3.0	Model (Å)
A residue					
ANH/A6	3.2	3.4	3.3	3.0	3.3
A2′/E2	2.5	2.5	2.6	2.5	2.4
-E1′	2.5	2.4	2.6	2.4	1.6
-A1′	2.7	2.8	2.8	2.8	2.6
-A2	2.8	2.9	2.8	2.8	2.7
DNH	2.6	2.9	3.0	3.0	2.0
A1′/A2	2.4	2.4	2.4	2.4	2.4
-E1′	3.2	3.0	2.9	2.9	4.1
-A6	3.4 (sd)	3.9	3.5 (sd)	3.5 (sd)	3.7
-Sal	2.7	2.7	2.7	2.6	2.6
A2/E1′	2.7 (Sal) (sd)	3.1	2.8 (sd)	2.9 (sd)	3.6
-E2	3.1 (sd)	3.3 (sd)	3.0 (sd)	3.1 (sd)	4.0
B residue					
BNH/F1′b	—	3.6 (ma)	3.6 (ma)	3.5 (ma)	2.2
-F1′a	—	3.4 (ma)	3.5 (ma)	3.4 (ma)	2.3
-B2	2.9	3.0	3.1	3.0	3.0
B1′/B2	2.5 (sd)	diag.	2.4 (sd)	diag.	3.4
-B6	3.0	2.9	2.8	2.9	2.9
-ENH	2.6	2.5	2.7	2.6	2.1
B2/C3	—	2.6	2.6	2.7	3.1
-C5 (Sgl)	3.5	3.0 (sd)	3.0 (sd)	3.0 (sd)	3.4
-C2	3.7 (sd)	3.0 (sd)	2.8 (sd)	3.1 (sd)	4.1
B6/E1′	2.8	2.9	2.8	2.9	2.8
-A5	3.0 (sd)	3.2	3.1 (sd)	3.0 (sd)	3.2
-ENH	3.3	3.1	3.1	3.1	3.3
-A2	3.6 (sd)	3.5 (sd)	3.2 (sd)	3.5 (sd)	4.1
-A6	(A5)	3.8 (sd)	3.2 (sd)	3.0 (sd)	4.1
C residue					
C2′/C1′	2.7 (a)	2.4	2.4	2.4	2.5
-C2	3.0	3.2	2.9	3.1	4.4
C1′/C2	2.7 (a)	2.4	2.5	2.4	2.4
-C6	—	4.2	3.7 (sd)	3.8	3.8
-C3	—	2.9 (sd)	2.6 (sd)	2.7 (sd)	4.7
D residue					
DNH/E2	3.0	2.9	3.0	2.8	1.9
-D1′	3.3	3.3	3.2	3.2	3.0
-A2	3.3	3.8	3.5	3.5	3.1
-E1′	3.2	2.9	3.0	3.0	3.1
D1′/D2	3.4	3.5	3.2	3.3	3.3
F residue					
FNH/F1′a	—	3.5 (ma)	3.4 (ma)	3.4 (ma)	
-F1′b	—	3.4 (ma)	3.3 (ma)	3.4 (ma)	
-F2′	3.6	3.3	—	—	3.0
F2′/F1′a	—	3.2 (ma)	2.9 (ma)	3.0 (ma)	
-F1′b	—	3.0 (ma)	2.8 (ma)	2.9 (ma)	
-F2(F6)	—	3.2	2.9	3.1	
F2(F6)/F1′a	2.3 (3.0)	3.1 (ma)	2.9 (ma)	2.9 (ma)	
-F1′b	—	3.1 (ma)	2.9 (ma)	3.0 (ma)	
G residue					
G1′/G2(G6)	3.3 (2.8)	3.0 (ma)	2.8 (ma)	2.9 (ma)	

[a] Solvent=DMSO-d_6 - H_2O; temperature=35°C[14~17].
[b] Solvent=DMSO-d_6; temperature=35°C.
[c] mt: Mixing time (mseconds).
[d] PD: Pulse delay (seconds).
sd: Spin diffusion, ma: motional averaging, a; for C1′α proton.
diag.: Signal intensity observed by diagonal peaks.

Table 3. NOE distance constraints for sugar residues[a].

Cross-peak	Actinoidin A (Å)				Actinoidin A_2 (Å)	
	mt[b] 300 PD[c] 15.0	mt 500 PD 2.5	Model		mt 500 PD 3.0	Model
D-Mannose (α-linkage)						
D4/Sm1	2.2	2.2	1.9		2.2	1.9
-Sm2	3.6	2.8	2.8		2.9	2.7
-Sm5(6)	3.6	3.0	5.1		3.6	5.1
Sm1/Sm2	2.6	2.5	2.6		2.5	2.6
-Sm5	3.8	3.1	3.7		3.0	3.7
D-Glucose (β-linkage)						
C5/Sg1(B2)	3.0	3.0	3.3		3.0	3.2
Sg1/Sg5	2.8	2.7	2.5		2.7	2.5
-Sg3	2.8	2.6	2.6		2.7	2.5
-Sg2	3.3	3.2	3.1		3.1	3.1
-Sa'1	3.6	3.5	3.1	-Sr1	3.4	3.2
Sg2/Sg4	(H_2O)	2.4	2.6		2.8	2.6
-Sa'1	2.7	2.6	2.7	-Sr1	2.5	2.6
Sg3/Sa'1	—	—	4.4	-Sr1	3.6	3.8
L-Acosamine (α-linkage) and L-rhamnose (α-linkage)						
Sa'1/Sa'2b	3.0	2.9	2.4		—	—
-Sa'2a	3.0	2.9	2.6	Sr1/Sr2	2.7	2.6
-Sa'3	—	3.6	3.8	-Sr3	3.1	3.8
-Sa'5	4.3	3.6	3.7	-Sr4	3.1	4.0
Sa'2a/Sa'2b	2.5	2.7	1.8		—	—
-Sa'3	3.2	3.2	2.5	Sr2/Sr5	2.3	2.5
-Sa'4	—	3.5	3.8	-Sr4	2.6	3.8
Sa'3/Sa'5	3.0	2.9	2.4	Sr3/Sr5	2.9	2.4
-Sa'4	3.1	3.3	3.1	-Sr4	Overlap	3.1
Sa'4/Sa'6	3.2	3.0	2.5~3.8	Sr4/Sr6	2.9	2.5~3.8
-Sa'5	3.5	3.3	3.1	-Sr5	3.9	3.1
Sa'5/Sa'6	2.7	2.6	2.5~3.1	Sr5/Sr6	2.7	2.5~3.1
L-Actinosamine (α-linkage)						
A2'/Sa1	—	3.8	4.6		3.7	4.6
A1'/Sa1	2.7	2.7	2.4		2.6	2.4
-Sa5	3.2	3.1	3.9		3.1	3.9
-Sa2a	4.1	3.7	4.3		3.7	4.3
A2/Sa1	3.6	3.2	3.9		3.3	3.9
A6/Sa1	2.9	2.9	3.3		2.9	3.3
-Sa2a	3.2	3.2	2.6		3.3	2.6
Sa1/Sa2b	2.8	2.8	2.4		2.8	2.4
-Sa2a	2.8	2.8	2.5		2.8	2.5
-Sa4	3.8	3.5	4.0		3.6	4.0
Sa3/Sa5	(H_2O)	2.6	2.5		2.8	2.5
Sa4/-OCH_3	2.8	2.7	2.5~3.6		2.7	2.5~3.6
-Sa5	3.5	3.2	3.1		3.2	3.1
-Sa6	3.0	2.8	2.6~3.8		2.9	2.6~3.8
Sa5/Sa6	2.7	2.6	2.5~3.1		2.6	2.5~3.1
-OCH_3	—	2.6	3.8~4.6		2.8	3.8~4.6
Sa6/-OCH_3	2.8	2.7	2.0~5.0		2.7	2.1~5.1

[a] All cross-peaks provide over-estimates of distance calculated from the model owing to motional averaging around the glycosidic bond which is not compensated for in the distance calculation.

[b] mt: Mixing time (mseconds).

[c] PD: Pulse delay (seconds).

and double quantum coherence experiments (DQCE) spectra which connect S6 to S5 and S5 to S4. The protons belonging to L-actinosamine (Sa) can be differentiated from those originating from L-acosamine (Sa′) by utilizing the NOE cross-peaks from the actinosamine S4-methoxy protons to Sa4 (δ 2.56) and to Sa6 (δ 1.16). Despite the limited information available at this point in assigning the carbohydrate proton signals, we were able to use it as a starting point in interpreting the information obtained in a homonuclear Hartmann-Hahn (HOHAHA) experiment. In the HOHAHA experiment as proposed by BAX, a MLEV-17 decoupling sequence is inserted between the evolution and detection period in a 2D NMR experiment. This creates isotropic mixing of magnetization among sets of *J*-coupled nuclei. This allows magnetization to be exchanged efficiently by traveling along a chain of *J*-coupled protons. The distance that the magnetization moves down the chain is dependent upon the coupling constants involved and the length of the mixing time. The HOHAHA offers several advantages over the COSY: 1) The effective *J*-coupling is doubled; 2) it yields multiplets which have all peaks in phase in contrast to a COSY experiment where partial cancellation may occur due to anti-phase cross-peak patterns and 3) magnetization decay rate is reduced where $T_1 > T_2$. This experiment proved extremely valuable for analyzing the sugars, since it was found that the spin magnetization moves rapidly around the carbohydrate rings during the mixing time. The only limitation being that the HOHAHA cross-peak reflects the magnitude of the coupling constants and so, small couplings on the

Fig. 3. 2D Proton-proton Hartmann-Hahn (HOHAHA) experiment of actinoidin A showing *J*-connectivities in each of the four carbohydrate components D-mannose (Sm), D-glucose (Sg), L-acosamine (Sa′) and L-actinosamine (Sa).

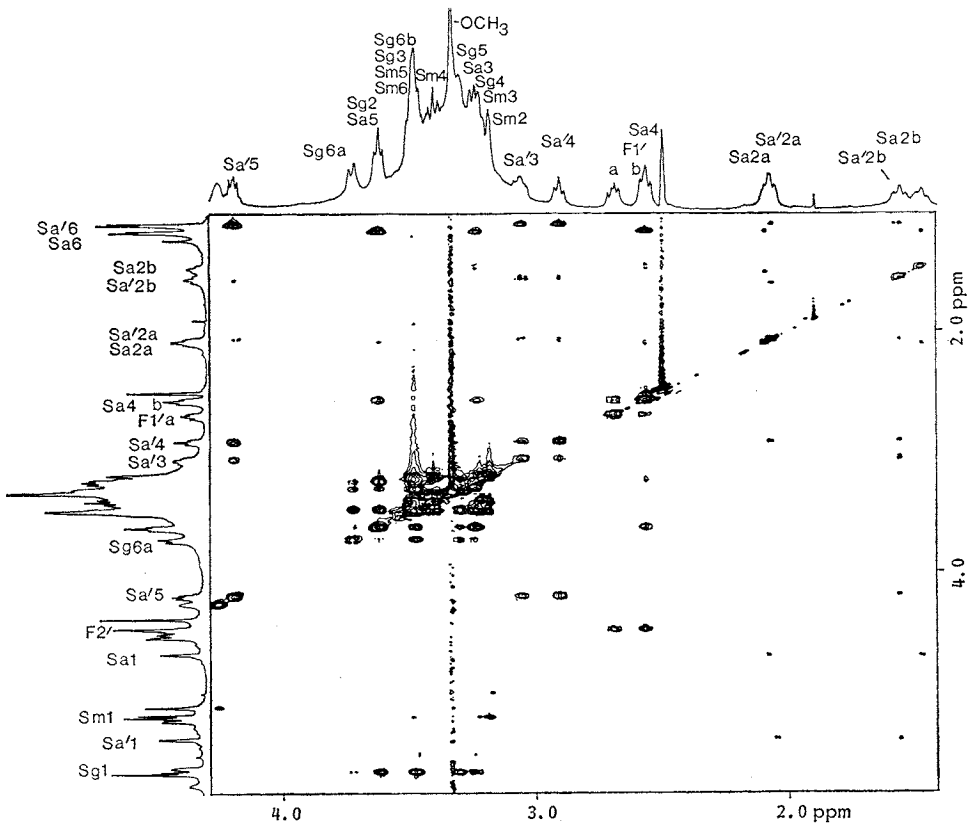

order of 1~2 Hz may hinder the transfer of magnetization. It was observed under the HOHAHA conditions at each frequency corresponding to the individual protons within a given carbohydrate ring, there are cross-peaks to all the other protons in that carbohydrate (see Fig. 3). In the HOHAHA spectrum starting with the S6 methyl signals in actinosamine at δ 1.16 and acosamine at δ 1.10, cross-peaks to S5, S4, S3, S2a and S2b in both sugar rings are readily observed. However, the small coupling constant between the geminal S2 protons and the S1 proton acts as somewhat of a bottle-neck to transfer of magnetization. Careful inspection of the spectrum reveals the existence of weak cross-peaks from the S2 protons in both sugars to the Sa1 and Sa'1 which are at δ 4.67 and δ 5.36, respectively.

The differentiation of the anomeric proton signals from the glucose and mannose residues was readily accomplished. In the case of glucose, sets of strong cross-peaks from each of the proton signals were found to all of the other ring proton signals whereas in mannose the Sm1 signal shows a cross-peak to Sm2 but not to any of the other protons; Sm2, Sm3, Sm4, Sm5, Sm6a and Sm6b all show mutual cross-peaks to each and every other proton in the set (see Fig. 3).

With all of the proton assignments secured by the HOHAHA, COSY and DQCE experiments, utilization of NOESY spectra to examine through space relationships from these protons could be employed to determine in conjunction with *J*-coupling the location and stereochemistry of the glycosidic linkages.

This is illustrated as follows: Sm1 shows strong NOE cross-peaks to D4 and Sm2 but no cross-peaks to Sm3 and Sm5, locating D-mannose at D5 as the α-glycoside. Sg1 shows an NOE signal to C5, placing the glucosyl residue at B4. The strong interaction between protons at Sg1 and Sg3 and Sg5 establish the axial nature of these hydrogens and identify its linkage as the β-glycoside in agreement with a *J* value of 8.3 Hz found for the Sg1 proton (see Table 1). In addition, NOE's are observed between D-glucose and L-acosamine in the disaccharide. Sa'1 yields a strong cross-peak to Sg2, and weak interactions to Sg1 and Sg3, confirming L-acosamine as the external sugar in the disaccharide through a glycosidic linkage at Sg2. The small value (J=1.2 and 2.3 Hz) of the *J*-couplings between Sa'1/Sa'2a and Sa'1/Sa'2 bprotons in conjunction with equally strong NOE cross-peaks observed between these protons indicate that L-acosamine is linked to glucose by an α-glycosidic bond. The existence of a strong NOE between Sg2 and Sa'1 in the disaccharide component, 2-(3-amino-2,3,6-trideoxy-L-*arabino*-hexopyranosyl)-β-D-glucopyranoside is most readily understood by contributions of the conformation shown in structure **3** in which in the particular rotamer shown, the two protons in question are in close proximity.

Finally, L-actinosamine can be positively located at the hydroxyl at A1'. Sa1 yields NOE signals to A1', A6, A2 and A5. The anomeric Sa1 proton also shows the same *J*-coupling and NOE pattern to Sa2a, Sa2b as observed for L-acosamine, which indicates that L-actinosamine is linked to A1' *via* an α-glycosidic bond. Following completion of this work the same conclusions regarding the stereochemistry and location of the carbohydrates in actinoidin A have been proposed on indirect evidence using ^{13}C shifts and ^{1}H-^{13}C coupling constants of model

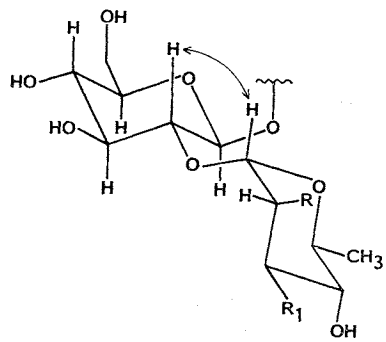

3 R = H $R_1 = NH_2$

4 R = R_1 = OH

glycosides[27].

Structure of Actinoidin A_2

For the protons in the heptapeptide core, actinoidin A_2 yields virtually identical NMR data to actinoidin A, supporting the chemically derived results which establish that the aglycones of actinoidins A and A_2 are indeed the same[12].

The four sugars, D-glucose, L-rhamnose, D-mannose and L-actinosamine, were assigned from a comparison of the COSY and double quantum coherence data of actinoidins A and A_2. Fig. 4 is a composite of the sugar regions from the COSY and DQCE spectra. The patterns in the spectra of the latter show characteristic differences in the sugar region from those observed for actinoidin A. The assignments of the L-actinosamine and L-rhamnose signals were again initiated from the S6 methyl signals at δ 1.19 and 1.08. Both sugars yield strong coupling cross-peaks connecting S6 to S5 and S5 to S4. Again, L-actinosamine is recognized from the observed NOE interactions between the S4-methoxy singlet and S4 and S6 (δ 1.19). Fortunately, the remaining frequencies associated with L-actinosamine yield strong coupling cross-peaks so that the anomeric proton, Sa1, is positively identified as the broad singlet at δ 4.73. The *J*-coupling trail for L-rhamnose leads directly into the complex sugar region. Connection of Sr4 to Sr1 is difficult to verify from the COSY data

Fig. 4. Proton-proton COSY (a) and double quantum correlation (DQCE) spectra (b) of actinoidin A_2 illustrating the assignment of the carbohydrate ring resonances.

Note that the overlap which occurs in the Sa4 and Sa5 signals in the COSY spectrum is resolved in the double quantum F_1 frequency axis in the DQCE spectrum.

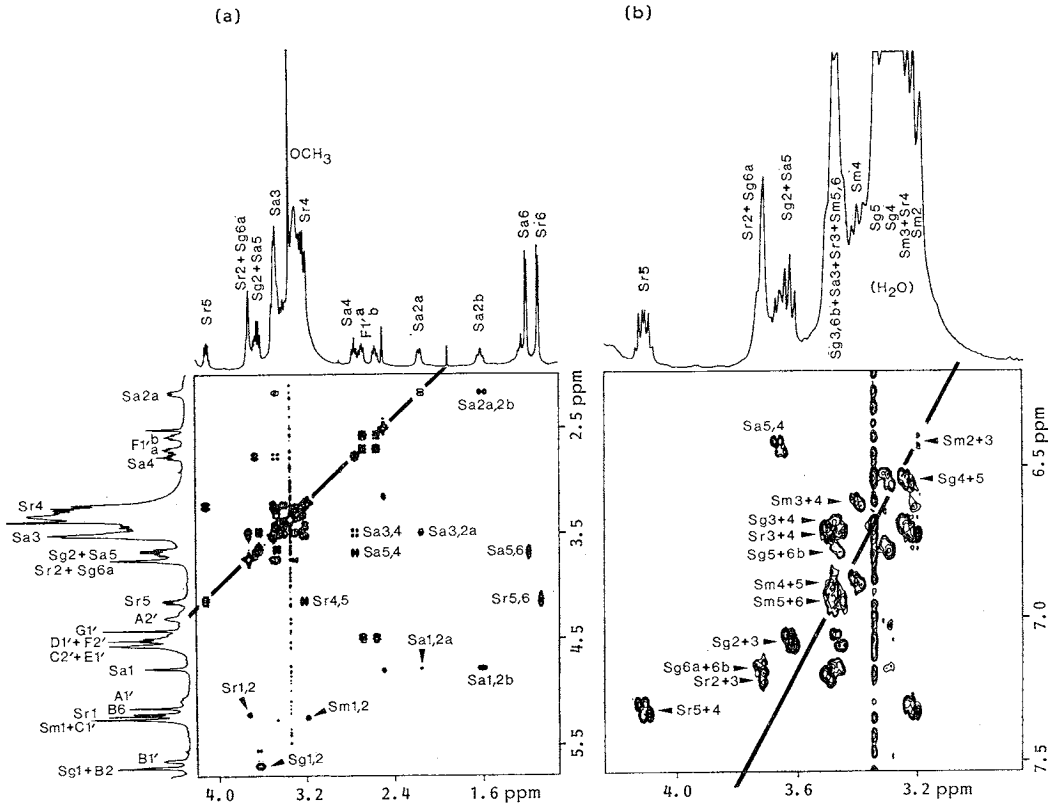

Fig. 5. Cross-section through the anomeric proton resonances of the carbohydrates in the 2D proton-proton nuclear Overhauser effect spectrum of actinoidin A_2.

The appearance of cross-peaks to C1′ and C2′ signals originates from overlap of the C1′ with the Sm1 signal.

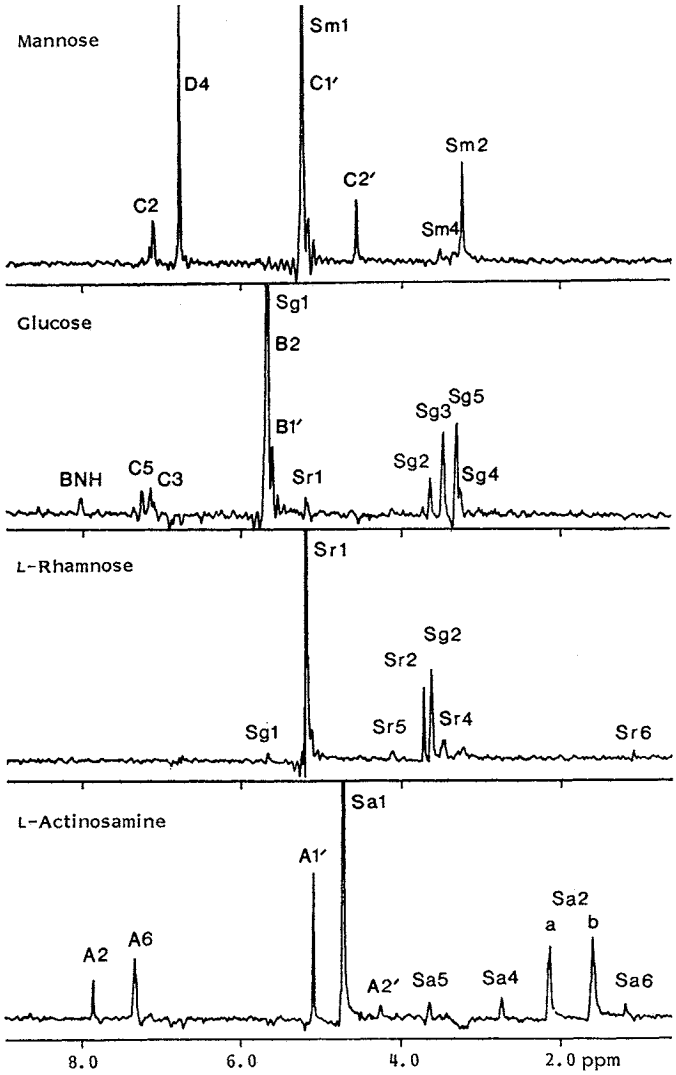

alone. The three remaining anomeric protons at δ 5.66, 5.20 and 5.17 are identified from their S1/S2 COSY cross-peaks. Careful inspection of the double quantum coherence and 2D NOE spectra allows each proton within a given sugar to be assigned. In fact, it is found that the chemical shifts for the protons in L-actinosamine, D-mannose (Sm1: δ 5.20) and D-glucose (Sg1: δ 5.66) are essentially unchanged from those observed in actinoidin A. The signals originating from L-rhamnose (Sr1: δ 5.17) provide the only unique differences. All assignments of the carbohydrate signals were readily confirmed by a HOHAHA experiment.

The location and configuration of the sugars is again determined from the 2D NOE spectrum of actinoidin A_2 in conjunction with *J*-coupling measurements of the anomeric protons. Fig. 5 shows the 2D NOE cross-sections through the anomeric protons. The patterns for glucose, mannose and

actinosamine are exactly the same as those described for actinoidin A. Therefore, their location and the configuration of the linkage is the same. The location and stereochemistry of the glycosidic link in rhamnose is clearly indicated from the anomeric proton signal in rhamnose which shows a weak *J*-coupling ($J<1.4$ Hz) and strong cross-peaks to Sg2 and Sr2, establishing its α-linkage to the 2-position of glucose. The presence of the latter NOE cross-peaks is again readily explained by contributions from a conformation in the disaccharide component corresponding to structure **4**. This completes the final detail of the structure of actinoidin A_2 which is represented by structure **1b**.

Conclusion

Previous ambiguities concerning the location of the chlorine substituent and the position and stereochemistry of the carbohydrate residues in actinoidin have been resolved.

The location of the chlorine at A3 rather than C3 which are the two alternates based upon earlier evidence[28,29] is clearly made from the NOESY data presented in Fig. 2. The use of the Hartmann-Hahn (HOHAHA) pulse sequence is shown to be particularly useful for assignment and characterization of the separate spin systems of each of the carbohydrate rings. NOESY cross-peaks from the anomeric proton peaks to aglycone protons in the heptapeptide core and between the anomeric proton (Sa'1) in acosamine and the Sg2 proton in glucose provides the remaining details of the structure of actinoidin A. A representation of actinoidin A is shown in structure **1a** where the disaccharide, 2-(3-amino-2,3,6-trideoxy-α-L-*arabino*-hexopyranosyl)-β-D-glycopyranosyl residue is at B4, the amino sugar, L-actinosamine is β-linked to the benzylic oxygen at A1 and D5 is the site for the β-D-mannosyl residue.

Parallel studies on the structure of the related antibiotic, actinoidin A_2 show that it differs from actinoidin A only in the structure of the disaccharide, 2-(6-deoxy-α-L-mannopyranosyl)-β-D-glucopyranoside at B4 in which L-rhamnose is present instead of L-acosamine. The structure of actinoidin A_2 is shown in **1b**.

Experimental

Materials

Actinoidins A and A_2 were isolated and purified from broths of a *Nocardia* sp. (SK&F AAJ-193) as described elsewhere[12].

Samples (8 mg) for NMR analysis were dissolved in 0.5 ml HPLC-grade water and the pH was adjusted to 7 using dilute CF_3COOH or NH_4OH. These were then lyophilized and dried by prolonged pumping in the presence of P_2O_5. Each resulting residue was dissolved in 0.5 ml freshly-opened DMSO-d_6 (100%).

NMR Spectroscopy

^1H NMR spectra were obtained on a Jeol GX500 spectrometer at 500.1 MHz. All 2D NMR data were transferred to a VAX 11/780 *via* magnetic tape and processed with software developed by D. HARE†.

Gaussian resolution enhancement was calculated on 1D spectra acquired under the following conditions: temperature=35°C; frequency=5,500 Hz; points=16,384; scans=1,000; Gaussian algorithm input: exponential factor=−5.0 Hz and Gaussian factor=0.5 Hz; reference=DMSO (2.49 ppm).

T_1-recovery times were measured from an inversion-recovery experiment utilizing the following conditions: temperature=35°C; frequency=4,201.7 Hz; points=4,096; scans=16; 6 intervals used: 1.0, 300, 800, 1,500, 2,700 and 6,000 mseconds; pulse delay=8 seconds; non-linear T_1-calculation performed on Jeol GX Version 4.1 software.

Details of the pulse sequences and phase cycling used for the COSY, DQCE and phase-sensitive

† D. HARE: Infinity Systems Design Inc., P.O. Box 15328, Seattle, WA 98115, U.S.A.

2D NOE experiments were described at length elsewhere[13~17]. In this work, the following conditions were utilized. The temperature was maintained at 35°C. The F_1 and F_2 spectral widths were set to 4,201.7 Hz. 2K sampling points were recorded in t_2 in the quadrature phase detection mode and 512 FIDs (zero-filled to 1K) were taken in t_1 (16 scans each). In the delayed-COSY experiment, the fixed interval before the mixing pulse was 200 mseconds and the delay before acquisition was 30 mseconds. The preparation interval in the DQCE experiment was 25 mseconds. In both experiments, unshifted sine-bell apodization was applied before Fourier transformation in both time domains.

The 2D HOHAHA pulse sequence involved a 90° pulse, a variable interval t_1 and a MLEV-17 sequence. The MLEV-17 sequence was repeated 29 times to yield a mixing period of 104 mseconds. The predriver (0.3 Watt) of the proton amplifier in the GX500 was used to generate the radio-frequency (rf) pulses. An rf field of 5 kHz was achieved. The HOHAHA spectrum was calculated in the phase sensitive mode using the method of STATES *et al.*[30], *i.e.*, 2 (1K) experiments for each of the 512 t_1-values. Zero-filling in F_1 gave a final 1 MWord square matrix.

In a 2D NOE experiment, the t_1 interval initiated at 0.01 msecond followed by mixing times of 300 or 500 mseconds with pulse delays of 3 or 15 seconds. A homogeneity spoiling pulse of 1 msecond was applied at the beginning of the mixing interval to suppress magnetization transfer due to *J*-coupling. All spectra were calculated in the phase sensitive mode using the method of STATES *et al.*[30]. F_2 contained 2K sampling points with 512 t_1-points recorded (zero-filled to 1K). No sine-bell enhancement was applied to the FIDs and the final matrices were not symmetrized.

Molecular Modeling

The actinoidins A and A_2 models were built from the starting geometry of the aridicin aglycone model whose construction has been described in detail[13]. The modifications were carried out on an Evans and Sutherland PS300 Graphics system linked to a VAX 11/785 computer and energy minimization carried out as previously described.

References

1) SHORIN, V. A.; S. D. YUDINSTSEV, I. A. KUNRAT, L. E. GOLDBERG, N. S. PEVZNER, M. G. BRASZHNIKOVA, N. N. LOMAKINA & E. F. OPARYSHEVA: New antibiotics, actinoidin. Antibiotiki 2: 44~49, 1957
2) WILLIAMS, D. H.; V. RAJANANDA, M. P. WILLIAMSON & G. BOJESEN: Part B. The vancomycin and ristocetin group of antibiotics. *In* Topics in Antibiotic Chemistry. Vol. 5. *Ed.*, P. G. SAMMES, pp. 119~158, Ellis Horwood Limited, Chichester, 1980
3) SZTARICSKAI, F.; C. M. HARRIS & T. M. HARRIS: Structural investigation of the antibiotic actinoidin: Identification of the tris (amino acid). Tetrahedron Lett. 1979: 2861~2864, 1979
4) LOMAKINA, N. N.; M. S. YURINA, Y. N. SHEINKER & K. F. TURCHIN: Structure of amino acids in ristomycin. Antibiotiki 17: 488~492, 1972
5) HARRIS, C. M.; J. J. KIBBY & T. M. HARRIS: The biphenyl constituent of ristocetin A. Tetrahedron Lett. 1978: 705~708, 1978
6) LOMAKINA, N. N.; V. A. ZENKOVA & M. S. YURINA: Absolute configuration of actinoidin amino acids. Khim. Prir. Soedin. 5: 43~46, 1969
7) SZTARICSKAI, F.; N. N. LOMAKINA, I. A. SPIRIDONOVA, M. S. YURINA & M. PUSKAS: Determination of carbohydrates in actinoidins A and B. Antibiotiki 12: 126~132, 1967
8) LOMAKINA, N. N.; I. A. SPIRIDONOVA, Y. N. SHEINKER & T. F. VLASOVA: Structure of the amino sugars from the antibiotic actinoidin. Khim. Prir. Soedin. 9: 101~107, 1973
9) SPIRIDONOVA, I. A.; M. S. YURINA, N. N. LOMAKINA, F. SZTARICSKAI & R. BOGNAR: Structure of the carbohydrate part of actinoidins A and B. Antibiotiki 21: 304~309, 1976
10) BERDNIKOVA, T. F. & N. N. LOMAKINA: Isolation and study of physicochemical properties of the products of a partial acid hydrolysis of the aglycon of actinoidin. Antibiotiki 21: 19~22, 1976
11) BERDNIKOVA, T. F. & N. N. LOMAKINA: On connection between carbohydrates with oxyaromatic amino acids in actinoidins A and B. Antibiotiki 22: 1077~1081, 1977
12) DINGERDISSEN, J. J.; R. D. SITRIN, P. A. DEPHILLIPS, A. J. GIOVENELLA, S. F. GRAPPEL, R. J. MEHTA, Y. K. OH, C. H. PAN, G. D. ROBERTS, M. C. SHEARER & L. J. NISBET: Actinoidin A_2, a novel glycopeptide: Production, preparative HPLC separation and characterization. J. Antibiotics 40: 165~172, 1987
13) JEFFS, P. W.; L. MUELLER, C. DEBROSSE, S. L. HEALD & R. FISHER: Structure of aridicin A. An in-

tegrated approach employing 2D NMR, energy minimization, and distance constraints. J. Am. Chem. Soc. 108: 3063~3075, 1986

14) HEALD, S. L.; L. MUELLER & P. W. JEFFS: Teicoplanin A_2: Structural analysis by 2D NMR. J. Mag. Res., 1986, in press

15) HUNT, A. H.; R. M. MOLLOY, J. L. OCCOLOWITZ, G. G. MARCONI & M. DEBONO: Structure of the major glycopeptide of the teicoplanin complex. J. Am. Chem. Soc. 106: 4891~4895, 1984

16) BARNA, J. C. J.; D. H. WILLIAMS, D. J. M. STONE, T.-W. C. LEUNG & D. M. DODDRELL: Structure elucidation of the teicoplanin antibiotics. J. Am. Chem. Soc. 106: 4895~4902, 1984

17) MALABARBA, A.; P. FERRARI, G. G. GALLO, J. KETTENRING & B. CAVALLERI: Teicoplanin, antibiotics from *Actinoplanes teichomyceticus* nov. sp. VII. Preparation and NMR characteristics of the aglycone of teicoplanin. J. Antibiotics 39: 1430~1442, 1986

18) BRAUNSCHWEILER, L. & R. R. ERNST: Coherence transfer by isotropic mixing: Application to proton correlation spectroscopy. J. Mag. Res. 53: 521~528, 1983

19) DAVIS, D. G. & A. BAX: Assignment of complex ^1H NMR spectra via two-dimensional homonuclear Hartmann-Hahn spectroscopy. J. Am. Chem. Soc. 107: 2820~2821, 1985

20) BAX, A. & D. G. DAVIS: MLEV-17-based two-dimensional homonuclear magnetization transfer spectroscopy. J. Mag. Res. 65: 355~360, 1985

21) AUE, W. P.; E. BARTHOLDI & R. R. ERNST: Two-dimensional spectroscopy. Application to nuclear magnetic resonance. J. Chem. Phys. 64: 2229~2246, 1976

22) BAX, A. & R. FREEMAN: Investigation of complex networks of spin-spin coupling by two-dimensional NMR. J. Mag. Res. 44: 542~561, 1981

23) MUELLER, L.: Mapping of spin-spin coupling via zero-quantum coherence. J. Mag. Res. 59: 326~331, 1984

24) MARECI, T. H. & R. FREEMAN: Mapping of proton-proton coupling via double-quantum coherence. J. Mag. Res. 51: 531~535, 1983

25) JEENER, J.; B. H. MEIER, P. BACHMANN & R. R. ERNST: Investigation of exchange processes by two-dimensional NMR spectroscopy. J. Chem. Phys. 71: 4546~4553, 1979

26) PACHLER, K. G. R.: Nuclear magnetic resonance (NMR) study of some α-amino acids. II. Rotational isomerism. Spec. Acta. 20: 581~587, 1964

27) BATTA, G.; F. SZTARICSKAI, J. CSANÁDI, I. KOMÁROMI & R. BOGNÁR: ^{13}C NMR study of actinoidins: Carbohydrate moieties and their glycosidic linkages. J. Antibiotics 39: 910~913, 1986

28) BERDNIKOVA, T. F.; N. N. LOMAKINA & N. P. POTAPOVA: Structure of the actinoidins A and B. Antibiotiki 27: 252~258, 1982

29) BERDNIKOVA, T. F.: Structure of the tricyclic triaminotricarboxylic acid (Y) from the antibiotic actinoidin. Antibiotiki 26: 816~820, 1981

30) STATES, D. J.; R. A. HABERKORN & D. J. RUBEN: A two-dimensional nuclear Overhauser experiment with pure absorption phase in four quadrants. J. Mag. Res. 48: 286~292, 1982